

^{90}Zr and ^{92}Zr : Neutron total and scattering cross sections*

P. Guenther, A. Smith, and J. Whalen

Argonne National Laboratory, Argonne, Illinois 60439

(Received 16 December 1974)

Total neutron cross sections of ^{90}Zr and ^{92}Zr were measured from 0.9 to 5.5 MeV and elastic and inelastic neutron scattering cross sections from 1.8 to 4.0 MeV. The inelastic neutron excitations of six states in ^{90}Zr and more than 12 in ^{92}Zr were observed. The experimental results formed the basis of an optical-statistical model interpretation including considerations of resonance width fluctuation and interference and the behavior of the optical potential near $N=50$. Comparisons of measured and calculated cross sections suggested new spin assignments for a number of excited states.

NUCLEAR REACTIONS $^{90,92}\text{Zr}$: measured neutron total and elastic and inelastic scattering cross sections, incident energy 1.8–4.0 MeV, deduced spins, parities, and nuclear model.

I. INTRODUCTION

The two isotopes ^{90}Zr and ^{92}Zr are situated at and just above the closed shell at $N=50$, respectively. In this region the density of excited states is changing rapidly, the s -wave strength function is near a minimum, and the p -wave strength function is large.^{1,2} An optical-model^{3,4} description of the neutron-nucleus interaction may be sensitive to both shell and isotopic effects^{5–8} as has been reported elsewhere.^{9–11} The properties of the excited states of ^{90}Zr are well established to excitations of more than 3.0 MeV Ref. (1) thereby reducing one source of uncertainties in statistical model calculations¹² and improving the potential for a detailed examination of the theoretical concepts.¹³ The latter are a matter of contemporary physical interest.¹⁴ One may expect considerable enhancement of energy-averaged cross sections for reactions in which the entrance and exit channel fluctuations are strongly correlated and a corresponding reduction in reactions without such correlations. In addition compound-nucleus inelastic neutron scattering cross sections should be enhanced by resonance correlations. These effects imply considerable corrections to the conventional Hauser-Feshbach formula.¹² Spectroscopic information for ^{92}Zr is incomplete at excitations ≥ 3.0 MeV and a comparison of measured and calculated neutron inelastic scattering cross sections can guide the selection of spin values.

Zirconium is a widely used structural material in fission-reactor systems. In these and other applications fast neutron cross sections of zirconium are of great importance.¹⁵ More than two-thirds of the element consists of the isotopes

^{90}Zr and ^{92}Zr . Therefore, these isotopes make the major contribution to the elemental cross sections. At low energies (≤ 1.0 MeV) the neutron total and elastic and inelastic scattering cross sections of the element are reasonably well known.^{16–18} However, as the energy increases into the few MeV range the knowledge becomes more uncertain. Cross sections for the scattering of 1.5 MeV neutrons from ^{90}Zr and ^{92}Zr have recently been reported by McDaniel *et al.*¹⁹ In addition, Stooksberry, Anderson, and Goldsmith²⁰ have reported a relative elastic scattering distribution for ^{90}Zr at 2.1 MeV.

The present program was undertaken in order to (a) provide nuclear data of great applied relevance, (b) examine the shell and isotopic dependence of the optical potential, and (c) phenomenologically explore the physical character of the compound-nucleus process.

II. EXPERIMENTAL METHODS

The samples employed in the measurements were right metallic cylinders 2 cm in diameter and 2 cm high. They were fabricated out of isotopically separated material enriched to greater than 95 at.%. The mass assay is given in Table I. There were negligible chemical impurities. Herein all cross sections are reported as barns per atom of the respective samples assuming 100% isotopic enrichment. Corrections for the effect of minority isotopes should be less than the experimental uncertainties. It was assumed that the samples were of uniform density and nondestructive tests indicated this was valid to within several percent. However, it was not possible

to destroy the samples for more precise assay. Sample nonuniformity could possibly effect the observed transmissions in the total cross section measurements and the effective angles in the differential scattering measurements.

All of the experimental measurements employed the intense-pulsed beam capability of the Argonne National Laboratory Tandem Dynamitron^{21, 22} and the ${}^7\text{Li}(p, n){}^6\text{Be}$ neutron-source reaction.²³ The burst duration was 1.0 ± 0.1 nsec at a repetition rate of 2.0 MHz. The lithium targets were vacuum deposited metal films the thickness of which was adjusted to obtain the desired incident neutron resolution.

The total cross section measurements were made using monoenergetic transmission techniques including fast time of flight for background and neutron-source control.²⁴ A massive shield and tapered collimator defined a beam of neutrons approximately 1 cm in diameter at the sample position. Source intensity was monitored with BF_3 counters appropriately placed internal to the source shield. The samples were mounted 2 m from the source on a rotating wheel with their cylindrical bases perpendicular to the neutron-beam axis. The sample wheel included the two zirconium samples, a carbon reference sample, and a void. A liquid-scintillation detector was placed approximately 5 m from the source on the beam axis. The time of flight of the neutrons to the detector was determined in a conventional manner using a time-to-amplitude converter. The time-of-flight resolution was 0.4 to 0.8 nsec/m, sufficient to amply separate the two neutron groups from the source reaction and primary neutrons from background contributions. The sample wheel was rotated at 30 revolutions per minute with the sample position synchronized with detector response. The data acquisition and reduction to cross sections was done in an automated manner using an on-line computer. The latter instrument was programmed to correct for background and carry the measurements through to the specified total cross section accuracy. Many aspects of these automated procedures have been defined in Ref. 25.

The scattering apparatus employed in the present work was an extension of that previously de-

scribed by Smith *et al.*²⁶ The number of detectors was increased from 8 to 10 (plus a monitor). The flight paths were increased from 2–3 m to 5–6 m with large increases in shielding. The diameter of the detectors was increased from 5 to 10 cm. The improved unit was installed at the Argonne Tandem Dynamitron in such a manner as to provide a detector angular range from -160° to $+160^\circ$. The samples were placed 13 cm from the neutron source with neutrons incident on their cylindrical sides. The collimator design was essentially as described in Ref. 26. The logic of the electronic circuitry has been previously outlined.²⁶ However, all electronic modules of the original system have been replaced with improved units. The contemporary installation was further discussed in Ref. 22.

The relative angular placement of the detection system was determined to better than 0.1° using a precision transit. The zero-angle position was determined by observing the relative energies of neutrons scattered from hydrogen both left and right of the center line using a single detector. The zero-angle position determined in this manner was reproducible to better than 0.5° . However, in a few instances the angular uncertainties could conceivably reach 1.0° . This maximum-limit estimate was inclusive of extreme variations in the illumination of the several millimeter diameter source spot. Actual variations were probably smaller as the particular accelerator used in this work is notable for high beam quality. At some angles and at the upper energies of the present work the general uncertainty in the zero-angle implies $\approx 3\%$ uncertainty in the differential elastic scattering cross section.

The primary neutron source monitor was a time-of-flight system collimated in such a manner as to view only the neutron source. The monitor system was integrated into the same on-line computer system handling the scattered neutron detectors. In addition, four "long counters" Ref. (27) were distributed about the neutron source in order to verify the response of the primary monitor. The primary monitor was the basis for correlating zirconium-sample, background, and hydrogen-calibration measurements. Its response rate was high with a consequent fractional percent statistical uncertainty.

Primary data were collected in an 8000-word digital computer.²⁸ A second identical unit was programmed and available as a backup. Several conventional pulse-height analyzers were employed for secondary data acquisition particularly associated with the optimization of time resolution. The computer data acquisition was in a multi-dimensional array with 16 energy recoil regions

TABLE I. Sample composition.

Sample	Isotope (at. %)				
	90	91	92	94	96
${}^{90}\text{Zr}$	97.72	1.07	0.51	0.56	0.15
${}^{92}\text{Zr}$	2.54	1.04	95.13	1.11	0.18

for each of the 10 scattered-neutron detectors. On-line processing included "walk" corrections²⁸ and the collapsing of the 16 regions into two predetermined sets generally corresponding to a "high" and "low" energy detector sensitivity. A variety of output options were available including graphical display and magnetic-tape dump. The scattered neutron velocity resolutions varied from 0.4 to 1.0 nsec/m depending on the selection of the energy regions and flight paths. The selection of resolution varied between measurements, and the same measurement could be analyzed with alternate choices giving emphasis to energy, sensitivity, resolution, signal-to-background, etc. Backgrounds varied from negligible values for high detector biases and prominent scattered neutron groups to as much as $\approx 20\%$ for low intensity groups and low detector biases. There were also wide variations in the statistical uncertainties associated with the observation of various neutron groups (e.g., less than 1% for a forward angle differential elastic cross section to 20% or more for a very minor and difficult to observe inelastic group).

The processing procedures were developed from the concepts outlined by Duffy, Buccino, and Smith²⁹ and Smith *et al.*²⁸ The data acquisition and processing procedures were integrated to provide an efficient flow of large blocks of information and particularly included extensive graphics procedures. The latter were essential to the effective handling of the more than 500 time-of-flight spectra involved in the present work. The time-of-flight peaks were integrated using visual judgments based upon line shapes determined from other measurements and the digital data base stored in an off-line 16 000-word digital computer.³⁰ Corrections were made for incident beam attenuation, angular resolution, and multiple-scattering effects within the samples. The latter were carried out with two special purpose Monte Carlo calculational programs.³¹ One of these (MONTE-POLY) corrected the observed scattering results from the CH_2 reference standard and was employed in determining both the relative detector sensitivities and their normalization. MONTE-POLY included a detailed treatment of the resonance cross sections of the carbon contained within the CH_2 sample. The second Monte Carlo program (MONTE-SAM) was used to correct the zirconium results and included a comprehensive treatment of both elastic and inelastic scattering processes. The Monte Carlo calculations led to uncertainties in the zirconium elastic scattering results of $\leq 3.0\%$ except at the minima of the diffraction patterns at higher energies where the uncertainty increased from 3–5%. The

Monte Carlo uncertainties associated with prominent zirconium inelastic neutron groups were $\leq 3.0\%$. Monte Carlo uncertainties associated with the CH_2 samples were $\leq 2.0\%$.

The relative detector efficiencies were individually determined for each of the 10 detectors by observation of neutrons scattered from CH_2 . The calibration was repeated at each of the five measurement periods. An incident neutron energy was selected 1.22 times the maximum energy of interest in the zirconium measurements (i.e., $1/\cos^2 25^\circ$). Each of the detectors was then set at 20–30 scattering angles distributed so that neutrons scattered from hydrogen had energies covering the entire range of interest for that measurement period. The yield of hydrogen scattered neutrons was determined at each of these angles and related to the known differential $\text{H}(n, n)$ scattering cross section³² to determine the relative detector sensitivities. It should be noted that the above determinations of relative sensitivities involved a fixed incident energy. They required that the neutron-source monitor be stable. They were not dependent upon a detailed knowledge of the source reaction or of the energy dependence of the monitor. The results were corrected as noted above. The resulting measured relative energy-dependent efficiencies were then least-square fitted with a power series the order of which was selected to smoothly interpolate between measured values. The average deviation of the measured values from the fitted curve was $\leq 3.0\%$ with the smaller deviations at the higher energies subsequently used in the normalization procedures. The detector energy-cutoff values varied from several 100 keV to 1 MeV depending on the quality of the given detector and the choice of bias value. The relative sensitivities were accepted for subsequent use only in a region of relatively slow energy dependence (e.g., neutron energies of ≥ 500 keV).

At each measurement energy, the normalization of each of the 10 detector sensitivities was established by observation of neutron scattering from the hydrogen of a CH_2 sample at a minimum of three scattering angles. The intensity of the observed scattered neutrons was related to the relative detector sensitivities at the respective neutron energies using the above power series fit to the relative sensitivity values. The normalization of each detector sensitivity was then established from the average of the measured values using the known differential $\text{H}(n, n)$ cross section.³² The results were corrected for perturbations due to incident beam attenuation, angular resolution, and multiple scattering as outlined above. It was assumed that the $\text{H}(n, n)$ reference

cross section was known to better than 1% in this energy range; therefore, its contribution to the present experimental uncertainties was ignored. The statistical uncertainties associated with the observation of scattering from hydrogen in the normalization procedures ranged from a fraction of a percent to 2.5% and the consistency of the normalization factors for a given detector and between detectors was $\approx 3\%$. A knowledge of monitor efficiency or relative energy-dependent sensitivity was not required by the above normalization procedures. With the normalization of the detector efficiencies the determination of the zirconium cross sections proceeded in a straightforward manner including the correction procedures outlined above.

It should be emphasized that, in many ways, the above procedures preserve the independence of the 10 detection systems. Thus experimental uncertainties in a given differential measurement were correlated to an appreciable extent with only one other differential value in a measured distribution and not propagated throughout the entire distribution. This implied that consistency throughout a distribution and between energies was a good measure of many experimental uncertainties. This was particularly so as the present results were obtained during five widely spaced intervals, each with different normalization measurements.

III. EXPERIMENTAL RESULTS

A. Total neutron cross sections

The total neutron cross sections of ^{90}Zr and ^{92}Zr were measured from 0.9 to 5.5 MeV at in-

tervals of ≈ 10 keV with resolutions in the range 5 to 10 keV. The results are summarized in Fig. 1.

The statistical uncertainty of the individual measurements varied from 2 to 5% with the large majority of uncertainties being $\approx 3.0\%$. Systematic uncertainties were estimated to be $< 3\%$. A primary systematic consideration was the potential non-uniform sample density. Concurrent measurements of the carbon total cross section were in agreement with those reported in the literature.³⁴ Above several MeV the total cross sections were relatively smooth functions of energy. However, below ≈ 1.5 MeV, particularly for ^{90}Zr , fluctuating, partially resolved structure becomes evident with increasing magnitudes with decreasing energy. Apparently, the only previous total cross section results directly comparable with the present work are the ^{90}Zr values of Stooksberry *et al.*²⁰ The agreement between the two sets of values is good as illustrated in Fig. 1. The ^{90}Zr scattering results at 1.5 MeV recently reported by McDaniel *et al.*¹⁹ are in very good agreement with the present total cross section results. The same authors report elastic and inelastic scattering cross sections for ^{92}Zr at 1.5 MeV that appear lower than those implied by the present total cross section results. However, either comparison is complicated by the presence of poorly resolved structure in the context of the respective experimental resolutions. Approximately, two-thirds of elemental zirconium consists of ^{90}Zr and ^{92}Zr . The relative-isotopic-weighted average of the present results is in good agreement with the reported total cross sections of the natural element.¹⁶ The

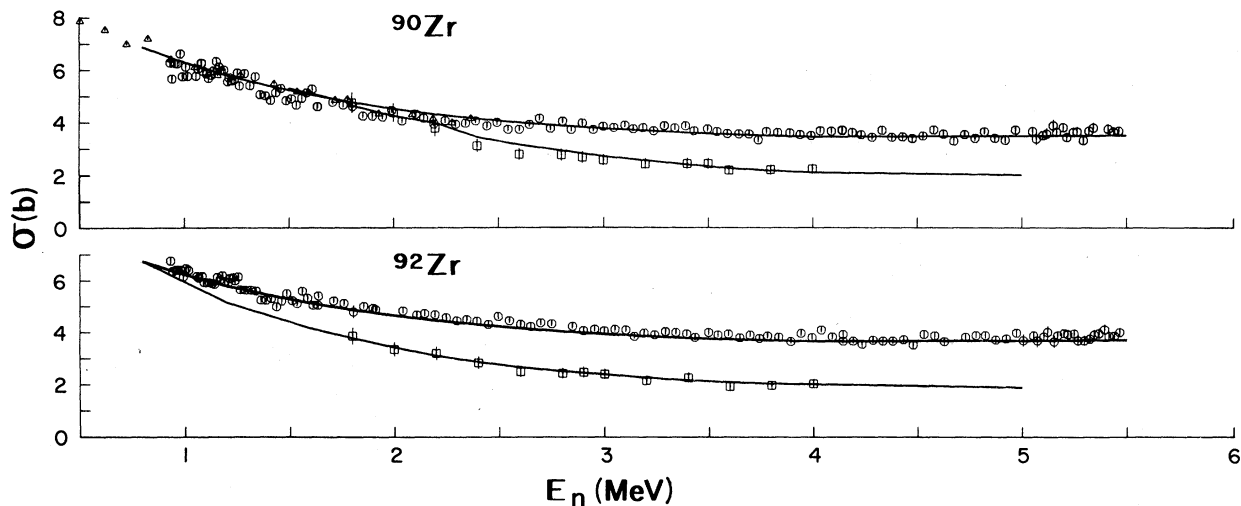


FIG. 1. Total and elastic scattering cross sections of ^{90}Zr and ^{92}Zr . The present results are indicated by circular (total cross sections) and square (elastic cross sections) data points. Triangles indicate the ^{90}Zr total cross section results of Stooksberry *et al.* (Ref. 20). Solid curves indicate the results of model calculations as described in the text.

present results do show a difference in total cross section magnitudes between the two isotopes. The difference is approximately that expected from a $R_0 A^{1/3}$ size effect.

B. Elastic neutron scattering cross sections

The differential elastic scattering cross sections were measured from 1.8 to 4.0 MeV at intervals of ≤ 0.2 MeV with energy resolutions of 30 to 50 keV. The measurements were made at 20 scattering angles distributed from $\approx 20^\circ$ to 155° . The experimental results are summarized in Fig. 2. All of these zirconium scattering cross sections were normalized to the $\text{H}(n, n)$ cross sections in the manner described above. Uncertainties due to counting statistics varied from a small fraction of a percent to $\approx 3\%$ in the diffraction minima of the higher energy distributions. Additional contributions to the total uncertainties associated with detector efficiencies and normalizations, angular definition, monitoring, and correction factors are discussed in the Sec. II, above. The total uncertainties varied with angle and energy. For approximately 90% of the differential cross section measurements, they were

in the range from 5 to 10%. The regions of primary exception were the diffraction minima where the differential cross sections drop from 10 to 15 mb/sr. In these areas it was subjectively judged that the total uncertainty was ≈ 2 mb/sr resulting in a relatively larger percentage uncertainty. Here, and generally, the uncertainty estimates were believed conservative. As noted in Sec. II, the experimental procedures were such that consistency within a given distribution and between many energies was a good indicator of many of the factors contributing to uncertainties. The consistency was well within the above estimates. Moreover, the differential scattering cross sections of carbon were routinely and concurrently determined with the zirconium measurements. The angle integral of the observed carbon cross sections was generally within 5% of the reported total cross sections³⁴ indicating that the over-all normalization of the detection system is consistent within the estimated uncertainties.

The angle-integrated elastic scattering cross sections were determined by least-square fitting the measured differential values with a Legendre polynomial series. Generally, there were no constraints on the fitting procedures. Particularly,

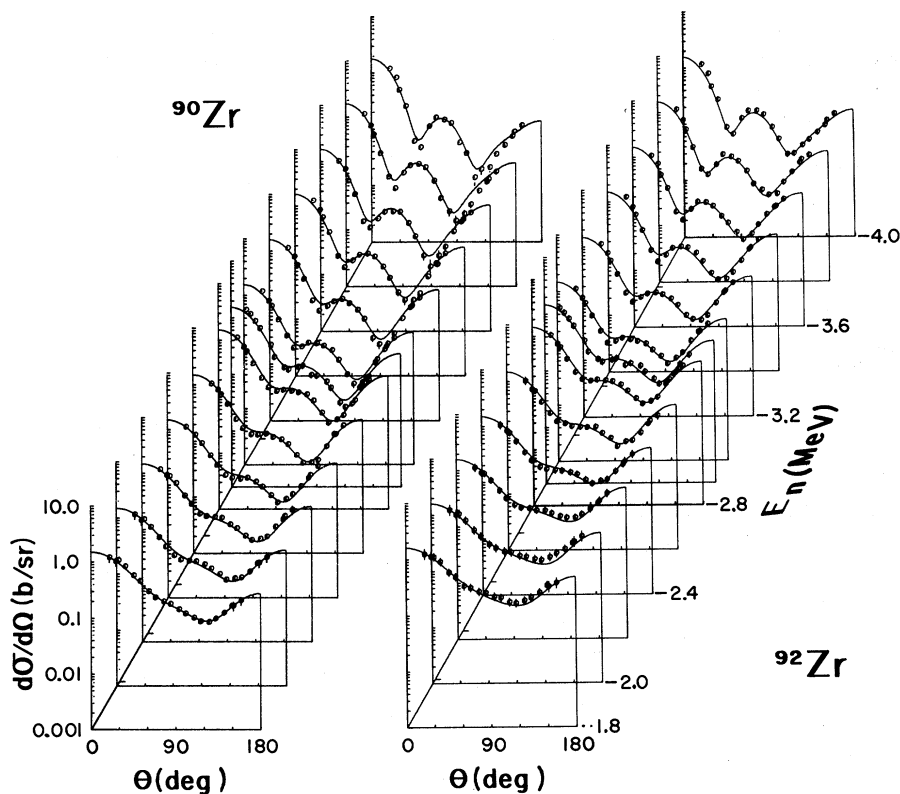


FIG. 2. Differential elastic scattering cross sections of ^{90}Zr and ^{92}Zr . The measured values are indicated by data points. Curves denote the results of optical-model calculations based upon average potentials as described in the text.

Wick's limit³⁵ or similar artifices were not employed to force the small-angle behavior. The resulting angle-integrated values are outlined in Fig. 1. The uncertainties in these angle-integrated cross sections were estimated to be 5 to 10% with the largest contribution due to the extrapolation from the most-forward measured point ($\approx 20^\circ$) to 0° . The angle-integrated ^{90}Zr elastic cross sections, combined with the inelastic scattering results (see below), led to total scattering cross sections whose deviation from the independently determined total cross sections over the entire energy range was 3.7%. The maximum deviation at any individual energy was 6.2%. Similar comparisons of the total scattering and total cross sections of ^{92}Zr resulted in deviations of 3.3% over the energy range 1.8 to 3.0 MeV and 5.1% over the entire energy range. These deviations are consistent with the respective experimental uncertainties despite the fact that some extrapolation of inelastic cross sections toward threshold was necessary in making these comparisons.

Comparable previous elastic scattering measurements appear confined to a single ^{90}Zr distribution reported by Stooksberry *et al.*²⁰ at 2.1 MeV. That experimental result apparently was arbitrarily normalized but it does have an angular-dependent shape consistent with the results of the present work. Very recently McDaniel *et al.*¹⁹ have reported elastic scattering results for ^{90}Zr and ^{92}Zr at a lower energy, 1.5 MeV. Their results appear to be reasonably consistent with an extrapolation of the present measurements.

C. Inelastic neutron scattering cross sections

The inelastic neutron scattering cross sections were determined concurrently with those for the elastic process using identical $\text{H}(n, n)$ calibration procedures as discussed in Sec. II, above. The optimum scattered neutron velocity resolution was sufficient to resolve most of the reported excited structure in these two isotopes. Cross sections were accepted when there was a reasonable response from five or more detectors generally implying a scattered neutron energy of greater than 0.5 MeV. Usually 15 to 20 data points were obtained on a given distribution. The various reaction Q values were determined from the known flight paths, flight times, and incident energies. These were verified by the observation of well known inelastic neutron processes (e.g., the excitation of the 0.846 MeV state in ^{56}Fe). The Q -value determinations were highly redundant and the final values were taken from a simple average of the measured quantities with the respective un-

certainties estimated from the consistency of the measured values. The resulting Q values were reasonably accurate but lacked the precisions obtainable using other spectroscopic methods (e.g., charged-particle and γ -ray spectroscopy as given in Ref. 1). The latter are generally preferred for analysis and are the values used in Sec. IV, below. The uncertainties in the measured inelastic cross sections varied with experimental conditions and the magnitudes and the locations of the respective scattered neutron groups. In the worst cases, uncertainties due to counting statistics were 20% or even more. The best of the differential inelastic results were uncertain to 5–10% percent inclusive of the various systematic factors discussed in Sec. II, above. The angle-integrated inelastic cross sections were obtained by least-squares fitting a Legendre polynomial series to the observed differential values. Most of the angular distributions were essentially isotropic. Exceptions were those associated with the excitation of the $0+$ states as illustrated by the ^{90}Zr example of Fig. 3.

Six inelastic neutron groups were observed in scattering from ^{90}Zr and more than 12 from ^{92}Zr . The excitation energies and the corresponding cross sections are summarized in Table II and Figs. 4 and 5. The spectroscopic character of these states is discussed in Sec. IV, below. The six states observed in ^{90}Zr closely correspond with those reported in the literature.¹ Only in the

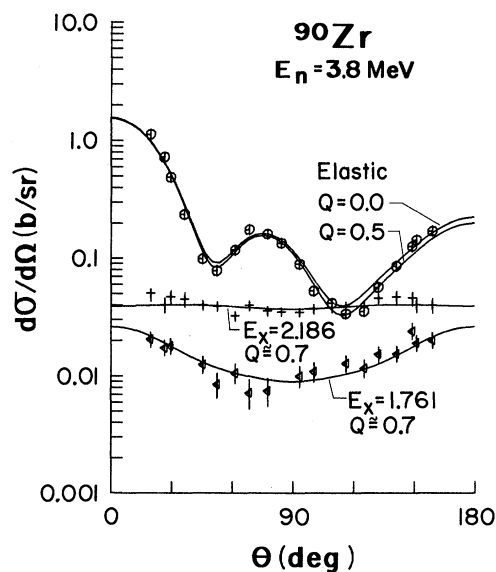


FIG. 3. The differential scattering of 3.8 MeV neutrons from ^{90}Zr . Data points indicate the present results for the noted excitation energies. The curves were obtained by calculation using the indicated values of the correlation parameter Q as described in the text.

case of the closely spaced 2738 and 2748 keV doublet did the present measurements fail to resolve all the reported levels. Apparently all previous inelastic neutron scattering studies of ^{90}Zr relied upon the γ -ray detection technique.³⁶⁻³⁹ This method does not always uniquely define neutron scattering cross sections. But even so, many of these γ -ray results are consistent with the present values to within the experimental uncertainties as illustrated in Fig. 4. Where there are pronounced discrepancies; they are attributable to the effects of γ -ray branching. Many of the neutron groups observed in neutron scattering from ^{92}Zr were clearly related to well established levels.¹ There was no evidence for the tentatively suggested state at ≈ 2.15 MeV.¹ The reported 2.34 and 2.39 MeV doublet was observed and also a single group corresponding to an excitation of ≈ 2.48 MeV. The latter has been suggested as a doublet with a few keV separation, well beyond the resolution of the present work. A single measurement implied a level at ≈ 2.66 MeV. A similar level has been previously suggested from (p, p') scattering measurements.¹ However, the

TABLE II. Observed inelastic neutron excitation energies in keV.

^{90}Zr		^{92}Zr	
Exp.	NDS ^a	Exp.	NDS ^a
1749 \pm 15(0+)	1761(0+)	934 \pm 10(2+)	934(2+)
2169 \pm 15(2+)	2186(2+)	1375 \pm 10(0+)	1383(0+)
2306 \pm 20(5-)	2319(5-)	1492 \pm 10(4+)	1496(4+)
2732 \pm 20(4-)+	2738(4-)+	1838 \pm 15(2+)	1847(2+)
	(3-)	2058 \pm 15(2+)	2067(2+)
	2748(3-)		
3068 \pm 20(4+)	3077(4+)	2320 \pm 20(3-)	2340(3-)
3300 \pm 20(2+)	3310(2+)	2360 \pm 20(1, 3)	2390(b)
		2486 \pm 20(5, b)	2480(b)
		2666 \pm 30(b)	2650(b)
		2778 \pm 30(2-3)	2740(b)
		2867 \pm 30(2-4)	2820(b)
		2851(b)	2851(b)
		2900 \pm 40(2-3)	2898(2, 3+)+
			2950(b)
		3063 \pm 30(b)	3040(2+)
		3187 \pm 30	3160+
			3174+
			3110+
			...
		3275 \pm 50	3223+
			3240+
			3264+
			3320+
			...

^a NDS refers to the *Nuclear Data Sheets* as defined in Ref. 1.

^b Uncertain or unknown J^π assignment as reported in Ref. 1 and/or deduced from the present work.

observed neutron cross sections were small and the present identification was considered very marginal. Neutron groups observed at excitations in the range 2.7 to 3.0 MeV were consistent with previous reported values, considering the energy resolutions of the present results. Above excitations of ≈ 3.0 MeV, the present results become more speculative. The experimental resolution was not comparable to the complexity of the reported structure and the observed cross sections were probably attributable to contributions from two or more states. There appear to have been only two previous direct measurements of inelastic neutron scattering from ^{92}Zr .^{19, 40} The results of Glazkov⁴⁰ are at a lower energy than those of the present work and the cross section is much lower than indicated by some ($n, n'\gamma$) measurements [e.g., the results of Day⁴¹]. The cross sections at 1.5 MeV recently reported by McDaniel *et al.*¹⁹ appear somewhat smaller than an extra-

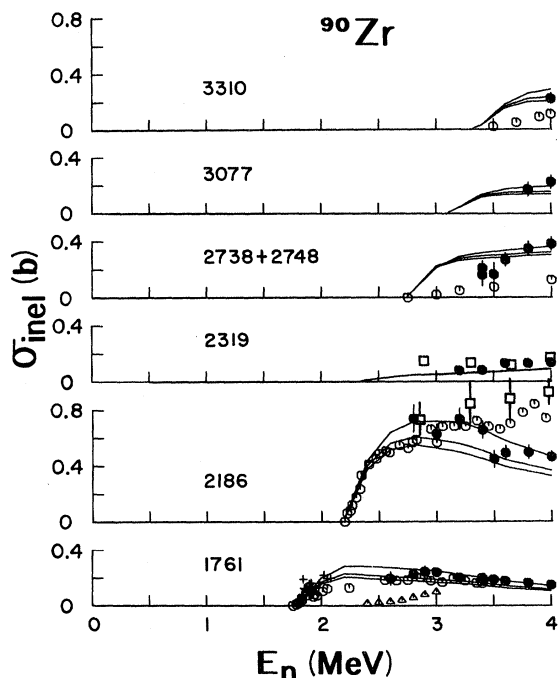


FIG. 4. Inelastic neutron excitation cross sections of ^{90}Zr . Solid data points indicate the present experimental results for the respective excitation energies (in keV). The results of comparable ($n, n'\gamma$) measurements are given: \circ , Lind and Day (Ref. 36); \triangle , Wagner *et al.* (Ref. 37); $+$, Tucker *et al.* (Ref. 38); and \square , Glickstein *et al.* (Ref. 39). These previous results are essentially γ -ray production cross sections. The curves are the results of calculations using correlation parameter, Q , values of 0.0, 0.5, and 1.0, respectively, the lower-, mid-, and upper-curve of each triad, as discussed in Sec. IV of the text.

polation of the present measurements and are possibly 20% lower than the results of $(n; n'\gamma)$ measurements by Day.⁴¹ Day⁴¹ and Tessler, Glickstein, and Carroll⁴² have extensively studied the $^{92}\text{Zr}(n; n'\gamma)$ process. The latter group gave particular attention to γ -ray cascades and branching ratios and derived neutron cross sections for a number of excitations. These agree with the present values to within the respective experimental un-

certainties. There is a similar agreement with the results of Day.⁴¹ Some of these comparisons are illustrated in Fig. 5.

IV. DISCUSSION

A. Optical model

The optical-model interpretation consisted of the derivation of an isotopically dependent potential from each of the experimental ^{90}Zr and ^{92}Zr data sets with subsequent inspection of the resulting parameters for evidence of isotopic, shell, and energy dependence as suggested and reported in previous work.⁵⁻¹¹ The resulting potentials were used for the subsequent interpretation of spectroscopic properties. The present measurements provided an auspicious foundation for such endeavors, with a good definition and scope extending over most neutron exit channels including both total and scattering cross sections in a sensitive mass-energy range. This is particularly so for ^{90}Zr where the properties of all states are reasonably known to excitations of ≤ 3.3 MeV.

The six optical-model parameters were determined from an χ^2 fit to each measured elastic scattering distribution over the energy range 2 to 4 MeV. The fitting procedures were inclusive of compound-elastic contributions calculated using the Hauser-Feshbach formula¹² corrected for width fluctuation effects.^{13, 43} The variations in the parameters for a given isotope were small, particularly if the few fits of lesser quality were omitted. The parameters were most uncertain at the lowest energies where the data were less reliable and at the highest energies (near 4.0 MeV) where all competing inelastic-neutron exit channels were not clearly known. The distribution of parameter values for a given isotope was generally random with no evident energy-dependent trend. The lack of any recognizable energy dependence was not surprising as studies based upon a far wider energy range indicate a relatively small energy dependence of the potential parameters. For example, the work of Engelbrecht and Fiedelney⁴⁴ implies a change from the average real-potential magnitude of +0.3 to -0.3 MeV going from incident energies of 2 to 4 MeV. These are small values, $\approx 0.6\%$ variations. The present total cross section measurements extend over a wider energy range than the elastic scattering values. Comparison of measured and calculated total cross sections in this wider context did suggest an energy dependence of the real potential consistent with that of Ref. 44. The final parameter sets for ^{90}Zr and ^{92}Zr were con-

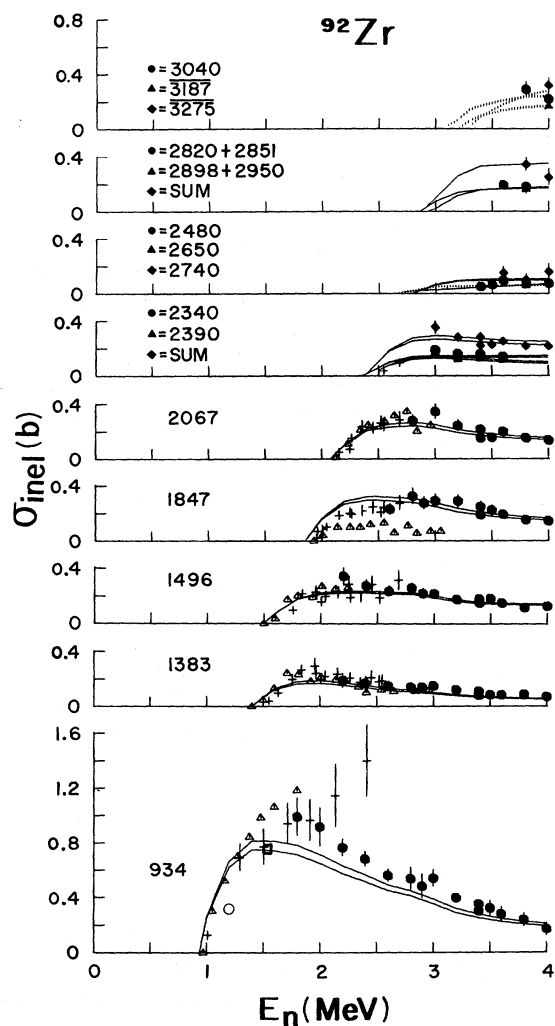


FIG. 5. Inelastic neutron excitation cross sections of ^{92}Zr . Solid data points indicate the present results for the respective excitation energies in keV. Previous results are indicated: \circ , Glazkov (Ref. 40); \square , McDaniel *et al.* (Ref. 19); \triangle , Day (Ref. 41); and $+$, Tessler *et al.* (Ref. 42). The latter two sets of data were obtained from $(n; n'\gamma)$ measurements. Curves indicate the results of calculations as described in the text. Where the curves are in pairs the lower one pertains to a correlation parameter $Q=0$ and the upper to $Q=0.5$. Elsewhere, single curves were obtained with $Q=0.0$.

TABLE III. Optical-model parameters.

^{90}Zr		
$V^a = 50.12 \pm 0.55^b$ MeV,	$R_v^c = 1.244 \pm 0.008$ fm,	$a_v = 0.600 \pm 0.055$ fm
$W^d = 5.50 \pm 0.48$ MeV,	$R_w^c = 1.250 \pm 0.075$ fm,	$b_w = 0.530 \pm 0.053$ fm
$V_{so}^e = 8.0$ MeV		
^{92}Zr		
$V = 49.50 \pm 0.50$ MeV,	$R_v = 1.238 \pm 0.005$ fm,	$a_v = 0.606 \pm 0.050$ fm
$W = 5.21 \pm 0.25$ MeV,	$R_w = 1.340 \pm 0.050$ fm,	$b_w = 0.550 \pm 0.042$ fm

^a Saxon real form.

^b All uncertainties are rms values derived from χ^2 six-parameter fits to the elastic angular distributions over the incident energy range 2.0 to 4.0 MeV as described in text. The estimates are very conservative.

^c All radii given in form $r = R_0 A^{1/3}$.

^d Saxon derivative imaginary form.

^e Thomas spin-orbit form fixed at the same magnitude for both isotopes.

structed of a simple average of the values obtained from the isotopic χ^2 fits. The results are summarized in Table III. The parameter uncertainties given in the table are the rms deviation from the average assuming equal weighting. These uncertainties are believed to be very conservative as they tend to be biased toward larger magnitudes by a few fits of less desirable quality.

Neutron total and elastic angle-integrated cross sections calculated with the potentials of Table III were in agreement with the measured values as illustrated in Fig. 1. In the low-energy limit the calculated $l=0$ strength functions were $\approx 0.6 \times 10^{-4}$ and consistent with systematic behavior in this mass region.² The two average potentials gave a very nice description of the observed elastic scattering angular distributions as illustrated by the curves of Fig. 2. Discrepancies between calculation and experiment were largest at lower energies and may represent true fluctuations in the measured data as is clearly evident in the neutron total cross sections at lower energies (see Fig. 1). All of these calculations included the width fluctuation correction.¹³ In addition, the ^{90}Zr results included resonance correlation corrections with the correlation parameter $Q = 0.5$. This additional correction did not have a large effect on the elastic scattering distributions and was relatively more important in the minima at higher energies as illustrated by the comparisons of Fig. 3. In these high energy areas, there are other uncertainties associated with the neglect of competition from unknown inelastic exit channels. Moreover, the correlation corrections are only approximations which, at higher energies with a number of channels, may break down and even lead to negative compound-elastic cross sections.¹⁴ Such anomalous behavior was observed for large values of the correlation parameter

(e.g., $Q = 1.0$) at 4.0 MeV. Despite these uncertainties, it is clear from the inelastic processes that such corrections are relevant as discussed below.

The potentials for ^{90}Zr and ^{92}Zr of Table III are essentially identical within estimated parameter uncertainties. Indeed the differences between the parameter values are less than would be expected assuming that the uncertainty estimates are equivalent to standard deviations. This fact tends to support the above premise that the uncertainties are conservative. Lane,⁷ Becchetti and Greenlees,⁸ and others^{4, 9, 11} have attributed an $[(N-Z)/A]$ dependence to the optical potential. This conclusion was deduced from basic physical concepts and phenomenological comparisons with measured data. In neutron processes the dependence leads to potential strengths of the form

$$V = V_0 - \left(\frac{N-Z}{A} \right) V_1 \text{ (real),} \quad (1)$$

$$W = W_0 - \left(\frac{N-Z}{A} \right) W_1 \text{ (imaginary),}$$

where $V_1 \approx 25$ MeV and $W_1 \approx 12$ MeV. These equations imply a difference between ^{90}Zr and ^{92}Zr real potentials of $\delta V \approx 0.49$ MeV and between imaginary potentials of $\delta W \approx 0.23$ MeV. Moreover, ^{90}Zr is at the closed shell $N = 50$ and Lane *et al.*⁷ and Vonach *et al.*⁶ have noted reduced optical-potential absorption as shell closures are approached. A similar effect has recently been suggested near $A = 100$ by Guenther *et al.*⁹ where comparisons of ^{92}Mo and ^{100}Mo neutron scattering results tend to indicate an approximately linear shell-dependent change of $\delta W \approx 1-2$ MeV over eight mass units. Thus, in the present context of neighboring ^{90}Zr and ^{92}Zr both the expected $[(N-Z)/A]$ and shell dependence of the potential

are equivalent to or smaller than the uncertainties in the parameter values given in Table III. Identification of such effects will probably require about a factor of 3 improvement in the accuracy of the parameter values. This will not be an easy task in this mass-energy range as the requisite experiments are very demanding and more critically, the fine details of the parameter selection will be influenced by compound-nucleus contributions. The detailed physical understanding of the latter is not certain and is now a matter of considerable theoretical discussion.^{14, 45, 46} Until these physical questions can be resolved and put into a useful computation form, it will be difficult, if not impossible, to determine compound-elastic components to accuracies necessary for the selection of potentials sensitive to small $[(N-Z)/A]$ and shell effects between nearby isotopes as in the present case.

B. Statistical model and spectroscopic parameters

The above optical-model parameters and compound-nucleus concepts were used to calculate the inelastic neutron scattering cross sections. The calculations employed the Hauser-Feshbach formula¹² with corrections for the width fluctuation and correlation of resonances. These corrections were implemented by means of the computer program NEARREX⁴³ using the Moldauer θ coefficients given by

$$\langle \theta \rangle = T + Q^{-1} [1 - (1 - QT)^{1/2}]^2, \quad (2)$$

where T are the conventional transmission coefficients and Q is the overlap parameter ranging from zero (for simple width fluctuation corrections) to unity.¹³ This expression is an approximate representation of the complex physical situation.¹⁴ It is qualitatively valid relatively near the inelastic reaction thresholds with a few open channels and will lead to the correlation enhancement of compound-inelastic cross sections. In the present calculations Q is treated as a free parameter, adjusted to obtain a phenomenological description of the observed cross sections.

The ⁹⁰Zr interpretation is relatively straightforward as the spectroscopic parameters of the excited states are well known¹ and the approximation of Eq. (2) is reasonably valid. The calculated cross sections for the excitations of the first two states [1.761 (0+) and 2.186 (2+) MeV] are sensitive to the choice of Q . Values of Q in the range 0.5 to 0.7 are reasonably descriptive of the observed inelastic neutron cross section and elastic scattering distributions as illustrated in Figs. 3 and 4. As more channels open, Q has less effect and the cross sections calculated with the reported

J^π values¹ and various values of Q are in reasonable agreement with the measured results as illustrated in Fig. 4. This agreement includes the unresolved doublet at an excitation of ≈ 2.74 MeV.

The interpretation of the ⁹²Zr results is more difficult as the spectroscopic character of the contributing states is not always known, more exit channels are open and the approximation of Eq. (2) becomes less valid. These complexities are not serious near the thresholds of the first two states [0.934 (2+) and 1.383 (0+) MeV] and comparison of measured and calculated results indicates Q values of 0.5 or larger as illustrated in Fig. 5. At higher energies (≈ 4.0 MeV) the calculations associated with the first two states using $Q \approx 1.0$ become unreliable as the approximations underlying Eq. (2) break down. Again the calculated excitations of the higher-energy excited states are not sensitive to the choice of Q . The J^π values of the 1.496 (4+), 1.847 (2+), 2.067 (2+), and 2.340 (3-) MeV states are well known¹ and the calculated cross sections in good agreement with observation. The J^π values of reported states at 2.39, 2.48, 2.65, 2.74, 2.82, and 2.85 MeV are uncertain.¹ A number of calculated results were compared with the present measured cross sections using a wide range of J values, proceeding in an iterative manner from lower to higher energies. The comparisons of measured and calculated values offer some guidance as to possible J values. Calculated results for the 2.39 MeV state using $J = 1$ or 2 agreed to within 35% with the average of measured cross section values. At some energies $J = 1$ gave a result within a few percent of the measured value. The measured cross sections for the inelastic excitation of the 2.48 MeV state are relatively uncertain and small. However, calculations based upon $J = 2, 3,$ or 4 resulted in cross sections more than a factor of 2 larger than the measured values and very much outside the experimental uncertainties. A $J = 5$ value has been suggested from proton scattering and (p, t) experiments.^{47, 48} Cross sections calculated with $J = 5$ are 80% larger than the present experimental results. The definition of the 2.48 MeV state is further confused by the possible presence of a second component at an excitation of 2.47 MeV.¹ Calculated excitations of the 2.74 MeV state assuming $J = 2, 3,$ or 4 agreed within $\approx 15\%$ with the average of the present measured values. Of these options $J = 2$ gave the best agreement ($\approx 7\%$ at some energies). Assuming a single state at 2.85 MeV, results calculated using J values of 2, 3, or 4 agreed to within $\approx 20\%$ with the observed cross sections. A similar single-state assumption and $J = 2, 3,$ or 4 resulted in calculated values accounting for more than 75% of the

observed cross section for the excitation of the 2.90 MeV state. Both the 2.85 and 2.90 MeV states have previously been reported as doublets (2.82-2.85 MeV and 2.90-2.95 MeV, respectively) which were not resolved in the present experiments.¹ The previous suggestions of $J = 2$ for the 2.85 MeV state⁴⁷ and $J = 2$ or 3 for the 2.90 MeV state¹ and the present work imply that the contribution to inelastic neutron scattering from the alternate member of each doublet is small (i.e., from the 2.82 and 2.95 MeV states). The observed state at 3.06 MeV was attributed to the reported 3.04 MeV (2+) level.¹ However, cross sections calculated under this premise were less than one-half the observed values. Thus, it is possible that the measured cross sections are in error or that there were additional components contributing to the observed cross sections for the excitation of this state. No attempt was made to calculate the cross sections for the marginally observed 2.666 MeV state. Neither was there any attempt made to correlate measured and calculated cross sections at excitation energies above ≈ 3.1 MeV because of the complexities and uncertainties in the experimental results, in the contributing structure and in the computational methods.

The above calculations can give guidance as to the relative energy dependence of the inelastic cross sections and, when correlated with measured values, assist in the assessment of spectroscopic parameters. However, the accuracy of prediction of inelastic cross section magnitudes near the first few thresholds, independent of experimental normalization, is no better than 20 to 30%. Such uncertainties are due to inadequacies in the basic understanding of resonance width fluctuations and correlations, and the associated computational techniques. These physical factors are contained in the "M" matrix of Refs. 13 and 14. Moldauer has pointed out the fortuitous property of the formulas to tend toward the familiar Hauser-Feshbach result at higher energies.¹⁴ The physical situation is not so simple in the region of the present experiments and is the subject of continued theoretical investigation by, for ex-

ample, Moldauer,¹⁴ Kawai, Kerman, and McVoy,⁴⁵ and Weidenmüller.⁴⁶

V. CONCLUDING REMARKS

The present measurements define the neutron total cross sections of ^{90}Zr and ^{92}Zr from below 1.0 MeV to 5.5 MeV and their neutron scattering cross sections from 1.8 to 4.0 MeV. These detailed results provide a foundation for the phenomenological interpretation of neutron processes in a mass-energy region where there is an interplay between direct and compound-nucleus reactions.

Optical potentials specifically appropriate to ^{90}Zr and to ^{92}Zr were deduced from the measured values. The respective potential-parameter sets were, within their small uncertainties, essentially identical. In particular, no significant $[(N-Z)/A]$ or shell dependence of the optical potential could be identified. Positive identification of such effects in the present energy-isotopic context will be exceedingly difficult as small variations in compound-nucleus mechanisms appreciably influence the model-parameter selection. The compound-nucleus process, particularly resonance width-fluctuation and correlation properties, may not be sufficiently understood to reliably determine optical parameters in this region to the necessary accuracies of better than a few tenths percent. Moreover, the computational tools for utilizing the theoretical concepts in experimental analysis are not generally available.

Comparison of measured and calculated neutron inelastic scattering cross sections demonstrated the importance of resonance width-fluctuation and correlation corrections to the simple Hauser-Feshbach formula. Parameter adjustment resulted in calculated cross sections descriptive of the experimental results. Correlation of measured and calculated neutron inelastic excitation cross sections give guidance to the selection of a number of previously uncertain spin values particularly those associated with states in ^{92}Zr at excitations of 2390, 2740, 2820, 2851, 2898, and 2950 keV.

*Work supported by the Energy Research and Development Administration.

¹*Nuclear Data Sheets*, A chains 90 and 92, compiled by J. Ball, H. Johns, and K. Way, (Academic, New York, 1966); D. Kocher and D. Horen, see *Nucl. Data*, A8, 407 (1970); *Nucl. Data* B7, 299 (1972).

²*Resonance Parameters*, compiled by S. Mughabghab and D. Garber, Brookhaven National Laboratory Report No. BNL-325 (1973), 3rd ed., Vol. 1.

³H. Feshbach, C. Porter, and V. Weisskopf, *Phys. Rev.* 90, 166 (1953).

⁴P. Hodgson, *The Optical Model of Elastic Scattering* (Clarendon, Oxford, 1963).

⁵A. Lane, J. Lynn, E. Melkonian, and E. Rae, *Phys. Rev. Lett.* 2, 424 (1959).

⁶W. Vonach, A. Smith, and P. Moldauer, *Phys. Lett.* 11, 331 (1964).

⁷A. Lane, *Phys. Rev. Lett.* 8, 171 (1962).

- ⁸F. Becchetti and G. Greenlees, *Phys. Rev.* **182**, 1190 (1969).
- ⁹A. Smith, P. Guenther, and J. Whalen, Argonne National Laboratory, Report No. ANL/NDM-7, 1974 (unpublished).
- ¹⁰D. Lind (private communication).
- ¹¹D. Velkley, D. Glasgow, J. Brandenberger, M. McEllistrem, J. Manthuruthil, and C. Poirier, *Phys. Rev. C* **9**, 2181 (1974).
- ¹²W. Hauser and H. Feshbach, *Phys. Rev.* **87**, 366 (1952); see also L. Wolfenstein, *Phys. Rev.* **82**, 690 (1951).
- ¹³P. Moldauer, *Phys. Rev.* **135**, B642 (1964). See also *Phys. Rev.* **123**, 968 (1961); *ibid.* **171**, 1164 (1968).
- ¹⁴P. Moldauer, *Bull. Am. Phys. Soc.* **19**, 988 (1974).
- ¹⁵Compilation of requests for nuclear cross sections, USNDC-6, 1972 (unpublished). Available from the National Technical Information Service, Springfield, Virginia.
- ¹⁶*Neutron Cross Sections*, compiled by M. D. Goldberg, S. F. Mughabghab, S. N. Purohit, B. A. Magurno, and V. M. May, Brookhaven National Laboratory Report No. BNL-325 (NTIS, Springfield, Virginia, 1966) 2nd ed., Suppl. 2.
- ¹⁷A. Langsdorf, R. Lane, and J. Monahan, Argonne National Laboratory Report No. ANL-5567 (Rev.), 1961 (unpublished).
- ¹⁸D. Reitmann, C. Englebrecht, and A. Smith, *Nucl. Phys.* **48**, 593 (1963).
- ¹⁹F. McDaniel, J. Brandenberger, G. Glasgow, and H. Leighton, *Phys. Rev. C* **10**, 1087 (1974).
- ²⁰R. Stooksberry, J. Anderson, and M. Goldsmith, Bettis Atomic Power Laboratory Report No. WAPD-T-2411, 1969 (unpublished).
- ²¹S. Cox and P. Hanley, *Bull. Am. Phys. Soc.* **60**, 221 (1971).
- ²²A. Smith, P. Guenther, J. Whalen, and P. Moldauer, *Bull. Am. Phys. Soc.* **18**, 312 (1973).
- ²³H. Newson and J. Gibbons, in *Fast Neutron Physics*, edited by J. Marion and J. Fowler (Interscience New York, 1963), Part 2, p. 1601.
- ²⁴D. Miller, in *Fast Neutron Physics*, edited by J. Marion, and J. Fowler (Interscience, New York, 1963), Part 2, p. 985.
- ²⁵J. Whalen, R. Roge, and A. Smith, *Nucl. Instrum. Methods* **39**, 185 (1966).
- ²⁶A. Smith, P. Guenther, R. Larsen, C. Nelson, P. Walker, and J. Whalen, *Nucl. Instrum. Methods* **50**, 277 (1967).
- ²⁷A. Hanson and J. McKibben, *Phys. Rev.* **72**, 673 (1947).
- ²⁸CDC-160A, Manufactured by the Control Data Corp., Minneapolis, Minn.
- ²⁹G. Duffy, S. Buccino, and A. Smith, Argonne National Laboratory, A Computer Program for the Processing of Fast Neutron Scattering Data, 1966 (unpublished).
- ³⁰SEL-840MP, Manufactured by Systems Engineering Laboratories, Fort Lauderdale, Fla.
- ³¹A. Smith and P. Guenther, *PARD*, Program for the Acquisition and Reduction of Neutron Scattering Data, Argonne National Laboratory Memorandum, 1973 (unpublished).
- ³²J. Hopkins and G. Breit, *Nucl. Data* **A9**, 137 (1971).
- ³³The numerical values of all experimental data reported herein have been transmitted to the National Neutron Cross Section Center, Brookhaven National Laboratory.
- ³⁴R. Schwartz, R. Schrank, and H. Heaton, National Bureau of Standards Report No. NBS-138, 1974 (unpublished).
- ³⁵See A. Lane and R. Thomas, *Rev. Mod. Phys.* **30**, 257 (1958), p. 293.
- ³⁶D. Lind and R. Day, *Ann. Phys. (N. Y.)* **12**, 485 (1961), see also Ref. 16.
- ³⁷R. Wagner, E. Shunk, and R. Day, *Phys. Rev.* **130**, 1926 (1963).
- ³⁸A. Tucker, J. Wells, and W. Meyerhof, *Phys. Rev.* **137**, B1181 (1965).
- ³⁹S. Glickstein, G. Tessler, and M. Goldsmith, *Phys. C* **4**, 1818 (1971).
- ⁴⁰N. Glazkov, *At. Energ.* **15**, 416 (1963).
- ⁴¹R. Day, as given in Ref. 16.
- ⁴²G. Tessler, S. Glickstein, and E. Carroll, *Phys. Rev. C* **2**, 2390 (1970).
- ⁴³Calculations employed the computer code NEARREX defined by P. Moldauer, C. Engelbrecht, and G. Duffy, Argonne National Laboratory Report No. ANL-6978, 1964 (unpublished).
- ⁴⁴C. Engelbrecht and H. Fiedeldey, *Ann. Phys. (N. Y.)* **42**, 262 (1967).
- ⁴⁵M. Kawai, A. Kerman, and K. McVoy, *Ann. Phys. (N. Y.)* **75**, 156 (1973).
- ⁴⁶H. Weidenmüller, *Phys. Rev. C* **9**, 1202 (1974).
- ⁴⁷J. Dickens, E. Eichler, and G. Satchler, *Phys. Rev.* **168**, 1355 (1968).
- ⁴⁸J. Ball, R. Auble, and P. Ross, *Phys. Rev. C* **4**, 196 (1971).